

Proteomic and Clinical Analysis of a Fine-Needle Aspirate Biopsy from a Single Cold Thyroid Nodule: A Case Study

Dijana Vitko^{1#} Fernando J. Sialana^{1,2#} Katja Parapatics¹ Oskar Koperek³ Christian Pötzi^{4,5} Shuren Li⁴ Keiryn L Bennett^{1*}

¹CeMM Research Center for Molecular Medicine of the Austrian Academy of Sciences, Vienna, Austria

²Department of Paediatrics and Adolescent Medicine, Division of General Paediatrics, Medical University of Vienna, Vienna, Austria

³Department of Clinical Pathology, Medical University of Vienna, Vienna, Austria

⁴Department of Biomedical Imaging and Image-guided Therapy, Division of Nuclear Medicine, Medical University of Vienna, Vienna, Austria

⁵Current address: Competence Centre for Thyroid Disorders, Vienna, Austria

*These authors contributed equally to the work

Abstract

Background: For cases where clinical and cytological data from cold thyroid nodules are ambiguous; pre-surgical proteomic profiling of fine-needle aspirate biopsies of cold thyroid nodules *in situ* can provide additional diagnostics to avoid invasive surgical intervention and thyroidectomy of benign or non-cancerous tissue.

Methods: The fine-needle aspirate biopsy lysate was digested with trypsin, and analysed by liquid chromatography mass spectrometry on a linear trap quadrupole Orbitrap Velos. Remaining peptides were separated by reversed-phase chromatography and fractions analysed as technical duplicates. Identified proteins were analysed by Gene Ontology and protein abundance were calculated using the Top3 label-free method. The proteomic data was complemented with ultrasonography and scintigraphy of the thyroid gland; and cytology of the cold thyroid nodule fine-needle aspirate biopsy.

Results: Sixty seven and 2,595 non-redundant protein groups (≥ 2 unique peptides) were identified from unfractionated and fractionated cold thyroid nodule fine-needle aspirate biopsy, respectively. Label-free protein abundance ranged over 6 orders of magnitude from the most abundant proteins, haemoglobin and thyroglobulin; to the low-abundance protein SON. Many previously-reported markers of thyroid cancer were in the top 23% of the identified proteins. Gene Ontology analysis revealed high-enrichment for cytoplasmic and membrane-bound organelle (cellular component); single-organism and small molecular processes (biological processes); and poly(A) ribonucleic acid, ribonucleic acid and protein-binding (molecular function).

Conclusions: The cold thyroid nodule was clinically-classified as benign. Proteomic data from fine-needle aspirate biopsies can provide additional diagnostic candidates indicative of a benign or cancerous cold thyroid nodule without the need for invasive surgical intervention.

Keywords: Thyroid nodule, FNAB, Cytology, Ultrasonography, Scintigraphy, Proteome, Orbitrap Velos

Abbreviations: AGC, automatic gain control; BCA, bicinchoninic acid; CID, collision-induced dissociation; CTN, cold thyroid nodule; DDA, data-dependent acquisition; FASP, filter-aided sample preparation; FNAB, fine-needle aspirate biopsy; LC-MSMS, liquid chromatography tandem mass spectrometry; LTQ, linear trap quadrupole; MALDI-MS, matrix-assisted laser desorption ionisation mass spectrometry; PAP, Papanicolaou stain; PBS, phosphate-buffered saline; SD, standard deviation; SPE, solid-phase extraction

Introduction

Cold thyroid nodules (CTN) are solid or fluid-filled masses that form within the thyroid gland. Clinical presentation following a scintigraphy shows reduced or no uptake of radionuclides. Most CTNs are symptomless and only 5-10% are malignant [1,2]. CTN is a common endocrine disorder, however, the molecular aetiology is unknown. The clinical concern is that hypofunctional lesions may be indicative of underlying cancer. Thus, a deeper understanding of CTN at the molecular level will aid diagnosis of thyroid carcinoma. Proteomic analysis of thyroid nodule fine-needle aspirate biopsies (FNAB) has the potential to deepen our knowledge on the molecular pathogenesis of CTNs; but only a few studies have been undertaken [3-6]. Excluding the one pre-surgical study [6], all are FNAB of tissue following total thyroidectomy. The four studies pooled 2-3 FNAB samples and coupled two-dimensional gel electrophoresis to MALDI-MS peptide mapping or MALDI-TOF-TOF-MSMS. Here we present a case report where a single biopsy from one *in situ* cold thyroid nodule was proteomically-profiled. The study was formally approved by the ethics committee of the Medical University of Vienna. The proteomic data

is complemented with thyroid ultrasonography and scintigraphy; and cytology of the FNAB.

Case Report

Materials and methods

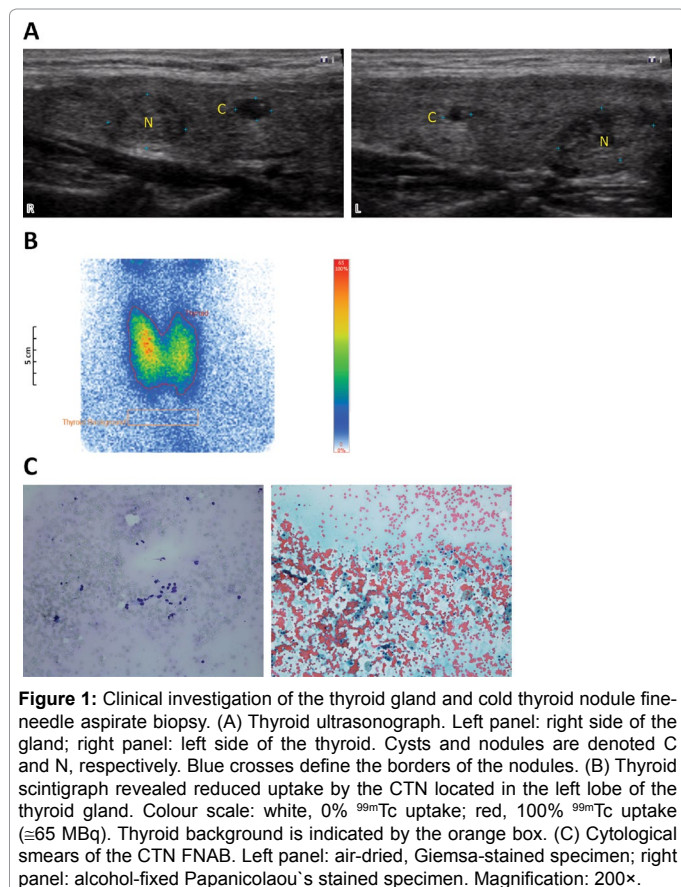
The ultrasonograph and scintigraph of the thyroid gland from a 44 year old woman; plus the cytological images of the CTN FNAB aspirated from the left lobe are shown in Figure 1. The ultrasonograph revealed the presence of cysts in both lobes of the thyroid gland (Figure 1A). In addition, the right and left lobes contain nodules measuring 1.1×0.5 cm and 1.2×1.8 cm, respectively. Scintigraphy was performed with 80 MBq of ^{99m}Tc (Figure 1B). The average uptake by the thyroid was 2.27%. The scintigraph shows an orthotopically-located, butterfly-shaped thyroid gland. Accumulation of the tracer is heterogeneous; and in the left lobe decreased retention of ^{99m}Tc is evident in the region of the nodule.

*Corresponding author: Keiryn L Bennett, CeMM Research Center for Molecular Medicine of the Austrian Academy of Sciences, Austria, Tel: +43-1-40160-70010; Fax: +43-1-40160-970000; E-mail: kbennett@cemm.oew.ac.at

Received January 21, 2016; Accepted April 20, 2016; Published April 25, 2016

Citation: Vitko D, Sialana FJ, Parapatics K, Koperek O, Pötzi C, et al. (2016) Proteomic and Clinical Analysis of a Fine-Needle Aspirate Biopsy from a Single Cold Thyroid Nodule: A Case Study J Clin Case Rep 6: 766. doi:10.4172/2165-7920.1000766

Copyright: © 2016 Vitko D, et al. This is an open-access article distributed under the terms of the Creative Commons Attribution License, which permits unrestricted use, distribution, and reproduction in any medium, provided the original author and source are credited.



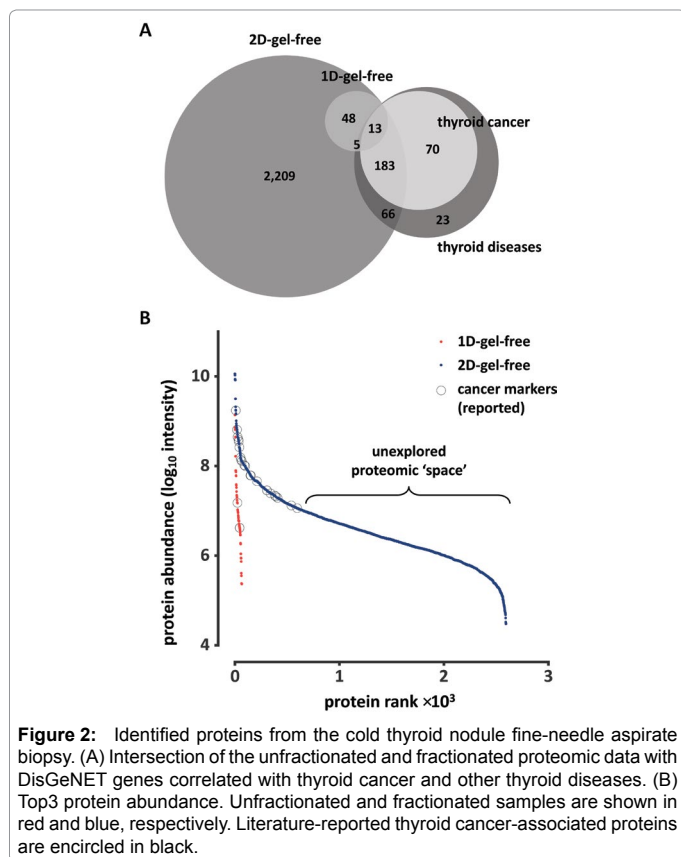
Guided by ultrasonography, a small, fine-gauge needle (23G) was inserted into the nodule from the left lobe (Figure 1A, right panel) and aspirate collected. The majority of the FNAB was used for cytological smears (Figure 1C); but the remainder was flushed from the syringe with PBS. After removal of most of the red blood cells, the FNAB was lysed in 100 μL 50 mM HEPES pH 8.0 (supplemented with 2% SDS, 1 mM PMSE, 1×protease-inhibitor cocktail); and the protein content determined. The lysate (50 μg) was processed by FASP [7, 8] and the resultant peptide equivalence of 2×500 ng protein was analysed by LC-MSMS on an LTQ Orbitrap Velos mass spectrometer (ThermoFisher Scientific, Waltham, MA) coupled to an Agilent 1200 HPLC nanoflow system (Agilent Biotechnologies, Palo Alto, CA) [9]. The remainder was separated into 10 HPLC fractions and analysed as technical duplicates. Detailed information on sample preparation, LCMS configuration and settings; raw MS data file conversion and protein database searches are provided in the supplementary material.

Results and Discussion

Excluding common contaminants (e.g., keratin, porcine trypsin), 67 and 2,595 non-redundant protein groups (≥ 2 unique peptides, including isoforms) were identified from the unfractionated and fractionated CTN FNAB, respectively (Supplementary Table S1). From DisGeNET [10], 360 genes were correlated with thyroid cancer and other thyroid diseases. Intersection of these genes with our data revealed the following. In terms of general thyroid disease, a total of 18 (27%) and 267 (11%) proteins from the unfractionated and fractionated samples, respectively, were common to the DisGeNET data (Figure 2A). More specifically, correlation of the samples with just the subset of thyroid cancer-associated genes revealed that 13 (20%) and 196 (8%) of the identified proteins intersected with the disease-associated data.

Protein abundance in the CTN FNAB was determined with the Top3 label-free method [11, 12] (Figure 2B, Supplementary Table S1). Unfractionated (red) and fractionated (blue) samples were plotted against protein rank order. Previously-reported thyroid cancer-associated proteins are encircled in black. Excluding haemoglobin, the two most abundant proteins were isoform 1 and 2 of thyroglobulin (THYG). THYG (~ 660 kD) is the extracellular, secreted glycoprotein precursor of the thyroid hormones tri-iodothyronine (T3) and tetra-iodothyronine (T4). Isoform 1 and 2 were identified with a total of 175 and 170 uniquely-identified peptides from 21,541 and 19,952 spectral counts and a sequence coverage of 60.8% and 60.2%, respectively. A minimum of 16 alternatively-spliced variants have been described for human THYG mRNA [13-16]. Differential splicing has been observed in normal, benign and malignant thyroid tissue; however, the presence of the isoforms do not appear to correlate with any underlying pathology [14]. In addition, post-translational modifications (PTMs) of thyroglobulin were apparent. The peptide VEAAATWYYSLEHSTDDYASFSR was observed in the unmodified form, and also with the addition of thyroxine and tri-iodothyronine on the tyrosine residue at position 2,573 (Supplementary Table S1). As far as we are aware, this is the first report where these PTMs have been identified on THYG by proteomics.

Despite the red blood cell lysis and removal from the biopsy material, several members of the haemoglobin family plus human serum albumin and other blood-related proteins were still highly-abundant. Nevertheless, many of the candidate proteins previously identified as indicators of thyroid cancer were present in the FNAB. These include: 6PGD, A1AT, ANXA1, APOA1, CATB, COF1, FRIH, FRIL, G3P, GRP78, HPT, LDHB, LG3BP, MOES, PARK7, PRDX1, PRDX2, PSME1, S10A6, SBP1, TTHY, VTDB [4-6, 17-19].



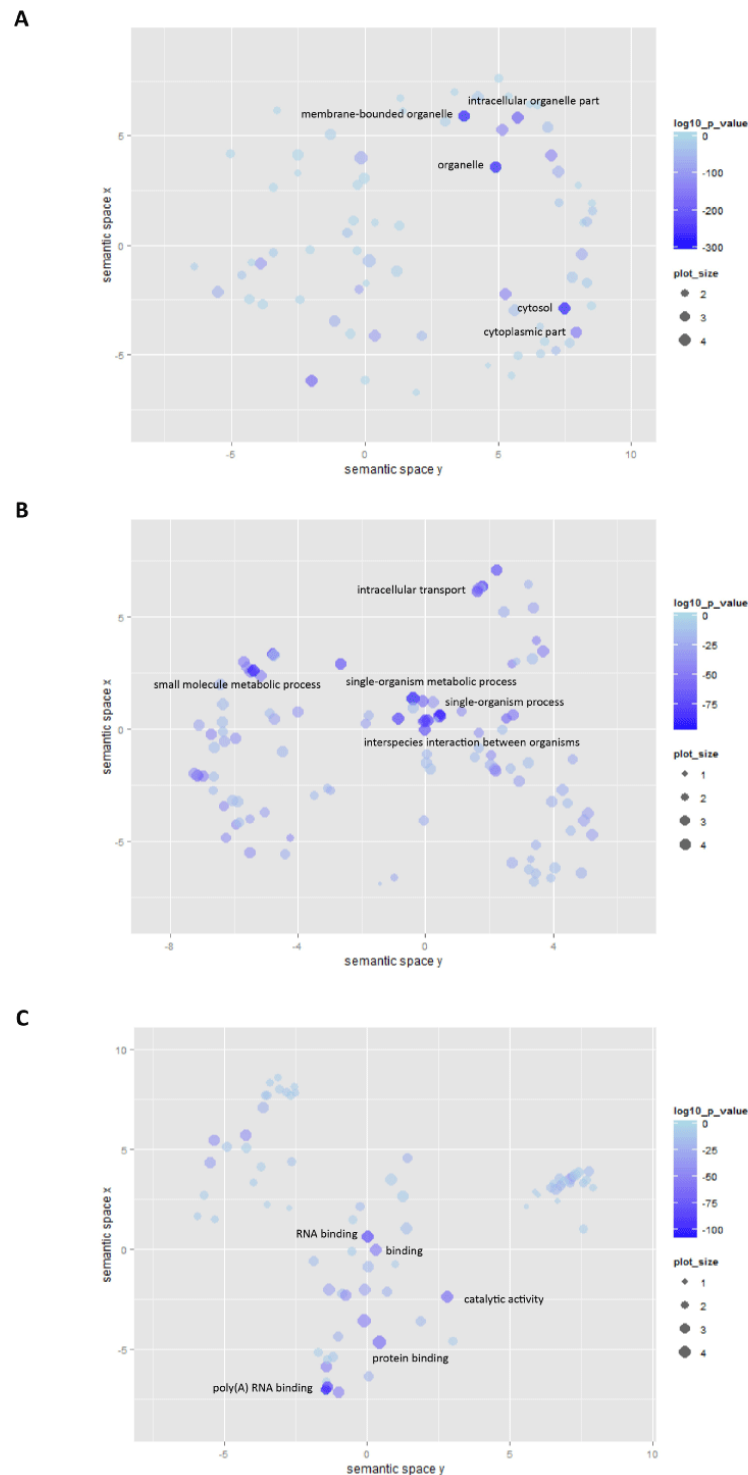


Figure 3: Revigo visualisation of the 2,595 proteins identified in the cold thyroid nodule fine-needle aspirate biopsy. GO terms for (A) cellular component, (B) biological processes, and (C) molecular function are given. The colour of the bubble indicates the significance of the GO term enrichment (low and high $\log_{10}P$ -values are more and less significant, respectively). The size of the bubble reflects the size of the GO term, i.e., the larger the bubble, the more genes clustered under a specific GO term. The five most significantly-enriched GO terms are depicted on each plot.

A1AT, CATB, FRIH, FRIL, G3P, GRP78, PRDX1, PRDX2 were identified in the unfractionated analyses; whilst all the previously-identified candidates were present in the top 23% most abundant proteins in the fractionated FNAB. Thus indicating that the studies performed to date are only sampling a small proportion of the thyroid

nodule proteome and that a large 'proteomic space' still exists in the analysis of FNAB (Figure 2B).

Analysis of all 2,595 identified proteins was performed with GOrilla [20] (P -value $\leq 10^{-6}$). GO term enrichment was performed

by searching the GO terms of the target list of genes compared to background, i.e., the entire human proteome (Supplementary Table S2). Using Revigo [21], enriched GO terms were visualised in semantic-similarity scatter plots. The 'simRel' score was chosen to assess the functional similarity of two GO terms [22] (Figure 3A-C). Cytoplasmic part and membrane-bound organelle were the most significant GO terms enriched for cellular component (\log_{10} P-values=-300 and -223.42); single-organism and small molecular processes for biological processes (\log_{10} P-values=-98.63 and -96.60); and poly(A) RNA, RNA and protein-binding for molecular function (\log_{10} P-values=-109.96, -96.22, and -94.31) (Supplementary Table S3).

The Giemsa-stained cytological smear was analysed microscopically and despite the blood cells, a high proportion of small- to medium-sized lymphocytic cells were evident (Figure 1C, left). In addition to individual, regressive, dissociated follicular cell monolayered sheets, there were single follicular cells and stripped nuclei. Single macrophages with some phagocytosed pigment were also present. The follicular cells were regressively-transformed with a slightly uneven distribution of the cytoplasm, and the nuclei were small and round but did not have any characteristics of papillary thyroid carcinoma. Individual histiocytic giant cells with phagocytosed pigment were also apparent. There were a low number of cells with further differentiated thyroid oxyphilic cytoplasm. A thin layer of aqueous protein-rich material was evident. The PAP-stained smear revealed regularly-structured squamous epithelia that were most likely due to contamination (Figure 1C, right). The clinical diagnosis of the single CTN FNAB was that the cystic thyroid material was significantly-differentiated, regressive but there was no indication of malignancy. According to the Bethesda 2009 classification [23], the nodule was diagnosed as benign.

In summary, we have proteomically-profiled a single FNAB of an *in situ* cold thyroid nodule that was clinically-diagnosed as benign. Our study shows that it is now possible to obtain a very deep proteomic analysis of FNAB. Thus, we believe that this advancement has the potential to assist in the diagnosis of thyroid cancer without the need for invasive surgery.

Acknowledgements

The authors would like to thank Marie L. Huber and Elisabeth Salzer from CeMM for the English translation of the clinical reports; and Professor Marcus Hacker from the Department of Biomedical Imaging and Image-guided Therapy, Division of Nuclear Medicine, Medical University of Vienna for encouraging the study. Research in our laboratory is provided by the Austrian Academy of Sciences.

References

1. Belfiore A, La Rosa GL, La Porta GA, Giuffrida D, Milazzo G, et al. (1992) Cancer risk in patients with cold thyroid nodules: relevance of iodine intake, sex, age, and multinodularity. *Am J Med* 93: 363-369.
2. Hegedüs L, Bonnema SJ, Bennedbaek FN (2003) Management of simple nodular goiter: current status and future perspectives. *Endocr Rev* 24: 102-132.
3. Giusti L, Iaconi P, Ciregia F, Giannaccini G, Basolo F, et al. (2007) Proteomic analysis of human thyroid fine needle aspiration fluid. *J Endocrinol Invest* 30: 865-869.
4. Giusti L, Iaconi P, Ciregia F, Giannaccini G, Donatini GL, et al. (2008) Fine-needle aspiration of thyroid nodules: proteomic analysis to identify cancer biomarkers. *J Proteome Res* 7: 4079-4088.
5. Iaconi P, Giusti L, Da Valle Y, Ciregia F, Giannaccini G, et al. (2012) Proteomic approach used in the diagnosis of Riedel's thyroiditis: a case report. *J Med Case Rep* 6: 103.
6. Ciregia F, Giusti L, Molinaro A, Nicolai F, Agretti P, et al. (2013) Presence in the pre-surgical fine-needle aspiration of potential thyroid biomarkers previously identified in the post-surgical one. *PLoS One* 8: e72911.
7. Wiśniewski JR, Zougman A, Nagaraj N, Mann M (2009) Universal sample preparation method for proteome analysis. *Nat Methods* 6: 359-362.
8. Manza LL, Stamer SL, Ham AJ, Codreanu SG, Liebler DC (2005) Sample preparation and digestion for proteomic analyses using spin filters. *Proteomics* 5: 1742-1745.
9. Bennett KL, Funk M, Tschernutter M, Breitwieser FP, Planyavsky M, et al. (2011) Proteomic analysis of human cataract aqueous humour: Comparison of one-dimensional gel LCMS with two-dimensional LCMS of unlabelled and iTRAQ(R)-labelled specimens. *J Proteomics* 74: 151-166. (PMID: 20940065)
10. Bauer-Mehren A, Rautschka M, Sanz F, Furlong LI (2010) DisGeNET: a Cytoscape plugin to visualize, integrate, search and analyze gene-disease networks. *Bioinformatics* 26: 2924-2926.
11. Cox J, Mann M (2008) MaxQuant enables high peptide identification rates, individualized p.p.b.-range mass accuracies and proteome-wide protein quantification. *Nat Biotechnol* 26: 1367-1372.
12. Silva JC, Gorenstein MV, Li GZ, Vissers JP, Geromanos SJ (2006) Absolute quantification of proteins by LCMSE: a virtue of parallel MS acquisition. *Mol Cell Proteomics* 5: 144-156.
13. Bertaux F, Noël M, Lasmoles F, Fragu P (1995) Identification of the exon structure and four alternative transcripts of the thyroglobulin-encoding gene. *Gene* 156: 297-301.
14. Bertaux F, Noel M, Malthiery Y, & Fragu P (1991) Demonstration of a heterogeneous transcription pattern of thyroglobulin mRNA in human thyroid tissues. *Biochem Biophys Res Commun* 178: 586-592. (PMID: 1859419)
15. Mendive FM, Rivolta CM, Moya CM, Vassart G, Targovnik HM (2001) Genomic organization of the human thyroglobulin gene: the complete intron-exon structure. *Eur J Endocrinol* 145: 485-496.
16. Targovnik HM, Cochaux P, Corach D, Vassart G (1992) Identification of a minor Tg mRNA transcript in RNA from normal and goitrous thyroids. *Mol Cell Endocrinol* 84: R23-26.
17. Brown LM, Helmke SM, Hunsucker SW, Netea-Maier RT, Chiang SA, et al. (2006) Quantitative and qualitative differences in protein expression between papillary thyroid carcinoma and normal thyroid tissue. *Mol Carcinog* 45: 613-626.
18. Krause K, Prawitt S, Eszlinger M, Ihling C, Sinz A, et al. (2011) Dissecting molecular events in thyroid neoplasia provides evidence for distinct evolution of follicular thyroid adenoma and carcinoma. *Am J Pathol* 179: 3066-3074.
19. Srisomsap C, Subhasitanont P, Otto A, Mueller EC, Punyarit P, et al. (2002) Detection of cathepsin B up-regulation in neoplastic thyroid tissues by proteomic analysis. *Proteomics* 2: 706-712.
20. Eden E, Navon R, Steinfeld I, Lipson D, Yakhini Z (2009) GOrilla: a tool for discovery and visualization of enriched GO terms in ranked gene lists. *BMC Bioinformatics* 10: 48.
21. Supek F, Bošnjak M, Škunca N, Šmuc T (2011) REVIGO summarizes and visualizes long lists of gene ontology terms. *PLoS One* 6: e21800.
22. Schlicker A, Domingues FS, Rahnenführer J, Lengauer T (2006) A new measure for functional similarity of gene products based on Gene Ontology. *BMC Bioinformatics* 7: 302.
23. Cibas ES, Ali SZ; NCI Thyroid FNA State of the Science Conference (2009) The Bethesda System For Reporting Thyroid Cytopathology. *Am J Clin Pathol* 132: 658-665.